Letter

Determining the nature of magnetism in altermagnetic candidate RuO_2

Tiema Qian,[1] Aya Rutherford,[2] Eun Sang Choi,[3] Haidong Zhou,[2] Boris Maiorov,[1] Minseong Lee,[1] and Christopher A. Mizzi[1,*]

[1]*National High Magnetic Field Laboratory, Los Alamos National Laboratory, Los Alamos, New Mexico 87545, USA*

[2]*Department of Physics and Astronomy, University of Tennessee, Knoxville, Tennessee 37996, USA*

[3]*National High Magnetic Field Laboratory, Tallahassee, Florida 32310, USA*

(Received 1 May 2025; accepted 10 February 2026; published 26 March 2026)

The terminology "altermagnetism" has recently been adopted to describe collinear magnetic order with no net magnetization and nonrelativisitic, momentum-dependent spin splitting. The archetypal material used to theoretically explore altermagnetism is RuO_2, but there has been significant debate as to whether RuO_2 possesses magnetic, let alone altermagnetic, order. To address questions surrounding the nature of magnetism in RuO_2, we combine symmetry-sensitive torque magnetometry and magnetization measurements in single crystals up to 31 T. The data are inconsistent with collinear magnetic order possessing a Néel vector along the *c* axis. Torque magnetometry further demonstrates an isotropic, field-independent magnetic susceptibility within the *ab* plane, indicative of neither a Néel vector within the *ab* plane nor a field-induced Néel vector reorientation. Magnetic quantum oscillations from both techniques reveal a nearly spherical Fermi surface pocket at the Brillouin zone center, in agreement with paramagnetic electronic structure calculations. Taken together, these data indicate that high-quality RuO_2 single crystals are itinerant paramagnets with no detectable long-range magnetic order and, by extension, no altermagnetism.

DOI: 10.1103/s98c-nkgj

Collinear magnetic systems have historically been classified as ferromagnets or antiferromagnets according to the magnetic moment density averaged over a magnetic unit cell [1]. Ferromagnets, with their finite magnetization and uniform spin splitting, have seen widespread application owing to their easy manipulation, but have size and speed limitations [2]. In contrast, antiferromagnets characterized by compensated magnetization and spin-degenerate electronic states have fast (∼THz) responses, but are more difficult to manipulate [3]. Recent analyses [4,5] based upon spin group theory [6] have led to the identification of a third class of collinear magnetic order that has zero net magnetization (like antiferromagnets) and spin splitting (like ferromagnets). These materials, often called "altermagnets" [4,5], are characterized by multipolar order parameters [7,8] and momentum-dependent spin splitting [9,10] arising from the spatial symmetry operations relating opposite spin sublattices. Importantly, spin splitting in altermagnets can be large (∼0.01–1 eV) owing to its nonrelativistic origin, making this class of materials promising for magnetic sensors and scalable data storage [4,5]. Furthermore, altermagnets may serve as platforms to realize phases such as those associated with Fermi liquid instabilities [11] and *p*-wave magnets [12].

A large body of research has emerged over the last few years examining the theoretical implications of systems exhibiting nonrelativistic, momentum-dependent spin splitting [4,5,13,14] and the experimental verification of altermagnetic properties [15–20]. Among the most studied materials in these contexts is RuO_2. Though it was first synthesized in the 1960s [21] and later developed as an electrode coating, catalyst, and low-temperature thermometer [22–24], RuO_2 has seen a resurgence of interest owing to its status as the archetypal altermagnet [4,5].

Despite serving as the prevalent theoretical model for altermagnetism, the crucial question remains: Is RuO_2 magnetically ordered? The first evidence for long-range magnetic order in RuO_2 was neutron diffraction measurements indicating that the system adopts a collinear antiferromagnetic structure with small moments ($\approx 0.05\mu_B$) along the *c* axis [25]. This result, in part, motivated the seminal works on altermagnetism and *ab initio* predictions of large spin splitting in RuO_2 [4,5]. While some issues with the interpretation of the neutron diffraction data have been raised [26], the central conclusion that RuO_2 has antiferromagnetic order was corroborated by follow-up resonant x-ray scattering measurements on both bulk and thin film samples (albeit with the possibility of slightly canted moments) [27]. Subsequent experiments on RuO_2 thin films provided further evidence for magnetic order including signatures of a magnetic transition in electrical transport, the presence of an anomalous Hall effect at high magnetic fields, and the identification of spin-split electronic bands with angle-resolved photoemission spectroscopy [19,27–34]. However, these findings are not universally observed in RuO_2 thin films [26,35] and additional

*Contact author: mizzi@lanl.gov

measurements on bulk RuO_2 are at odds with the neutron and x-ray results: Thermodynamic, transport, and optical measurements do not observe an antiferromagnetic transition, muon spin rotation spectroscopy does not find signatures of a spontaneous internal magnetic field, and angle-resolved photoemission spectroscopy does not resolve spin-split electronic states [26,35–45].

Amid these discrepancies, the existence of (alter)magnetic order in RuO_2 remains an open question. Further, if RuO_2 is magnetically ordered, it is ambiguous whether the origin is intrinsic (i.e., the magnetic ground state of bulk RuO_2) or extrinsic (i.e., stabilized by strain, defects, etc.). High magnetic field studies of bulk RuO_2 single crystals with thermodynamic probes of magnetic anisotropy are singularly suited to resolve these questions. First, if ordered moments exist in RuO_2, it is clear their magnitude is minute and high magnetic fields will amplify their signatures. Additionally, high magnetic fields are known to have a pronounced impact on the magnetic anisotropy in other rutile antiferromagnets owing to field-induced rotations of the Néel vector [46]. While consequences of this effect have been observed in RuO_2 thin films [19,28], there are no direct measurements of magnetic anisotropy in bulk RuO_2 single crystals up to high magnetic fields; such measurements are crucial to determine whether the putative magnetic order is intrinsic. Finally, de Haas-van Alphen quantum oscillations [47] in high magnetic fields enable a quantitative connection between sample quality and magnetic order in a single measurement. The former is derived from the Dingle temperature and sensitivity of quantum oscillations to small volume fractions of additional grains, domains, and/or secondary phases. The latter is because the spin-split electronic states in altermagnetic RuO_2 are predicted to cause large Fermi surface anisotropies (e.g., [48]).

In this Letter, we combine high magnetic fields with symmetry-sensitive, thermodynamic measurements to ascertain the nature of magnetism in RuO_2 single crystals. Our approach, rooted in symmetry, combines multiple techniques with reproduced findings on multiple samples to simultaneously assess evidence for and against magnetic order. First, we leverage the sensitivity of torque magnetometry (a probe of magnetic susceptibility anisotropy) and comprehensive models of the effects of magnetic order on the magnetic susceptibility tensor to determine that only magnetic order characterized by an isotropic, field-independent magnetic susceptibility within the *ab* plane and a larger, field-independent susceptibility along the *c* axis are consistent with experiment. To distinguish between the remaining possible forms of magnetic order, we combine these symmetry constraints with quantitative arguments derived from magnetization measurements that indicate RuO_2 is an itinerant paramagnet at all measured temperatures and magnetic fields. We confirm this interpretation by demonstrating close correspondence between the theoretical Fermi surface of paramagnetic RuO_2 and the experimental Fermi surface determined from magnetic quantum oscillations.

In Fig. 1, we examine the form of the magnetic susceptibility tensor (which describes the magnetization arising from a magnetic field to lowest order) for the rutile crystal structure with different magnetic orders [49]. Scenarios in which a rutile crystal is either paramagnetic (Case I) or altermagnetic

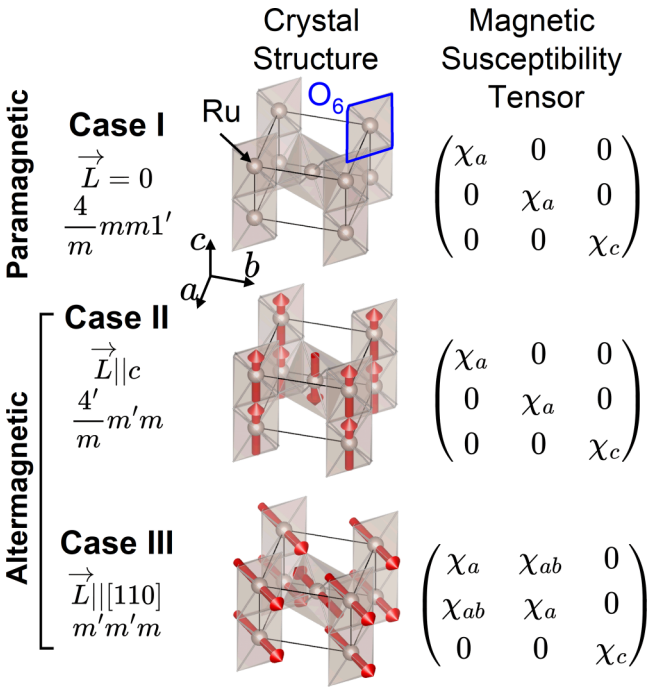

FIG. 1. Three possible magnetic states in RuO_2. Case I is paramagnetic and Cases II and III are different altermagnetic orders. The direction of the Néel vector ($\vec{L}$), magnetic point group, crystal structure, and magnetic susceptibility tensor are provided for each case. Tensors are given with respect to the tetragonal axes of the parent paramagnetic structure.

with the Néel vector along the *c* axis (Case II) allow for uniaxial magnetic anisotropy with an isotropic magnetic response within the *ab* plane (χ_a) and a distinct response along the *c* axis (χ_c). Case II is the most commonly reported magnetically ordered ground state for RuO_2 (e.g., [19,25]). Magnetic susceptibility has the same form in Cases I and II because a Néel vector along the *c* axis maintains tetragonal symmetry. If the Néel vector was in a direction other than the *c* axis, the symmetry of the system would be lower than tetragonal allowing for additional independent magnetic susceptibility components. One such example is Case III, where the Néel vector is along [110]. Case III has been reported for RuO_2 thin films [19,28] and CoF_2 single crystals [46] at high magnetic fields. However, this possibility has not been explored with thermodynamic measurements in single crystal RuO_2 under high magnetic fields. Other scenarios, including noncollinear magnetic structures, are considered in the Supplemental Material [50].

It follows that the experimental determination of the magnetic susceptibility tensor will constrain the magnetic state in RuO_2. Toward this end, we use a direct, sensitive, and thermodynamic probe of small anisotropies in magnetic susceptibility: torque magnetometry [51]. Magnetic torque measurements consist of rotating the magnetic field within a crystallographic plane and measuring the torque normal to that plane (Fig. 2). As shown in the Supplemental Material [50], an easy axis in a direction other than the *c* axis would, at a minimum, cause a finite torque for magnetic fields rotated within the (001) plane and differences in the torque

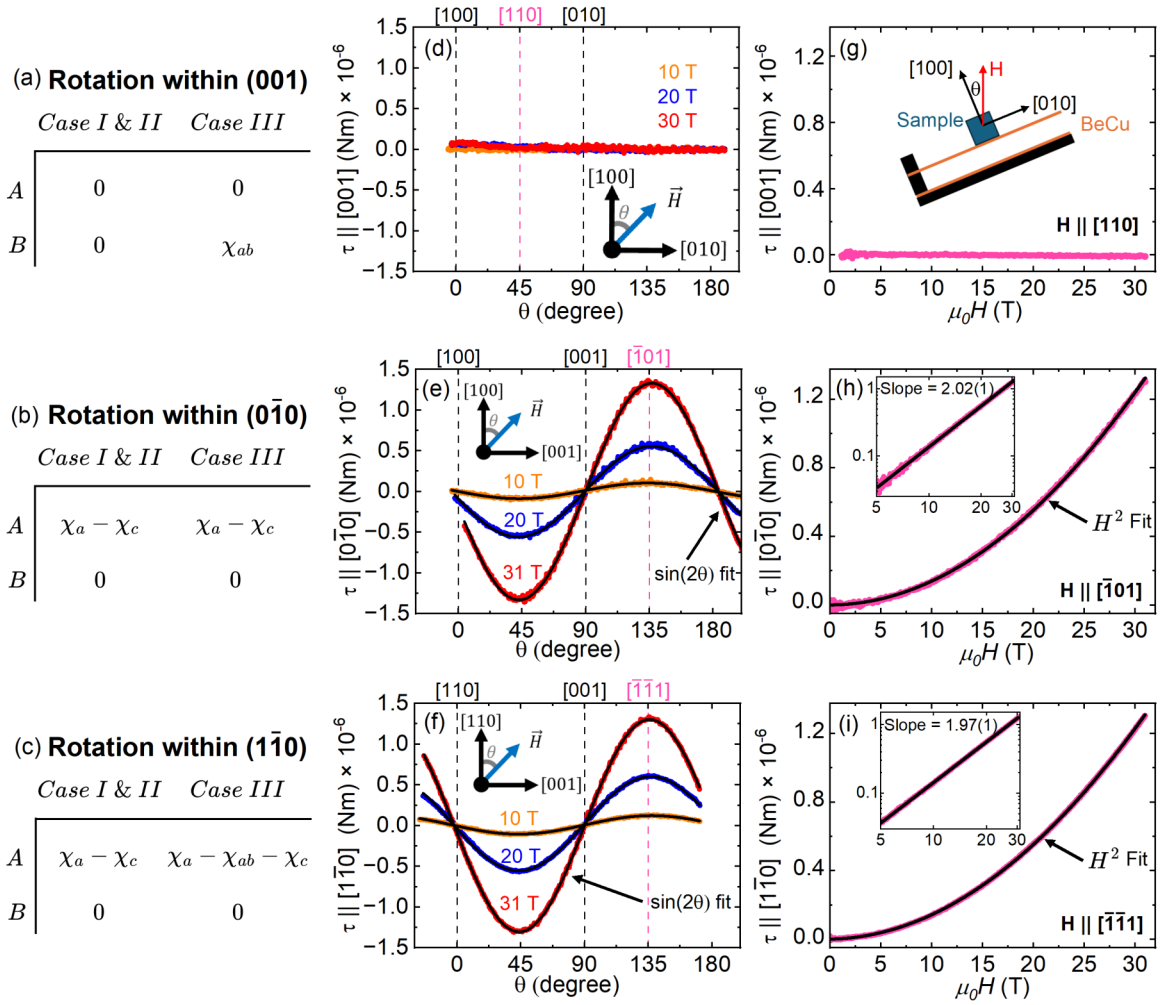

FIG. 2. Torque magnetometry on a RuO_2 single crystal at 40 K. (a)–(c) Torque expressions for Cases I–III (Fig. 1) for the three measurement configurations described in the text. A and B are coefficients in $\tau(\theta) = \mu_0^2 H^2[\frac{A}{2}\sin(2\theta) + B(2\sin^2(\theta) - 1)]$. (d)–(f) Angular-dependent torque for rotations of the magnetic field within the (001), (0$\bar{1}$0), and (1$\bar{1}$0) planes. Data for the (d) (001) configuration are not periodic, whereas data for the (e) (0$\bar{1}$0) and (f) (1$\bar{1}$0) configurations are described by a $\sin(2\theta)$ form. (g)–(i) Field-dependent torque amplitude for fixed directions within the (001), (0$\bar{1}$0), and (1$\bar{1}$0) planes. Data for the (g) (001) configuration do not have a measurable field dependence up to 31 T, whereas data for the (h) (0$\bar{1}$0) and (i) (1$\bar{1}$0) configurations scale quadratically with magnetic field. Insets of panels (h) and (i): Log-log fitting of torque amplitude showing quadratic scaling. A schematic of the experiment is shown in (g).

response for fields within the (0$\bar{1}$0) and (1$\bar{1}$0) planes (see expressions in Fig. 2). Magnetic domains would also affect the magnetic anisotropy by changing the periodicity of the torque (e.g., torque measurements on MnTe with domains [52]). Thus, experimental configurations were adopted to rotate the magnetic field within the (001), (0$\bar{1}$0), and (1$\bar{1}$0) planes.

Figures 2(d) and 2(g) demonstrate that rotating the magnetic field within the (001) plane produces no discernible torque up to 31 T (see the Supplemental Material for details [50]). In contrast, rotating the magnetic field within the (0$\bar{1}$0) and (1$\bar{1}$0) planes yields identical torque responses up to 31 T: For a fixed magnetic field, the torque in both configurations has the same sinusoidal dependence on angle with an equivalent amplitude and periodicity of 180°. Furthermore, Figs. 2(h) and 2(i) show that the torque amplitudes do not deviate from field squared scaling within these two planes. Note, data in Fig. 2 were taken at a single temperature (40 K) because the magnetic susceptibility magnitudes and anisotropy only weakly depend on temperature (Fig. 3), and the effects of quantum oscillations are minimized at 40 K (Fig. 4).

The three angular and field dependencies in Fig. 2 are only simultaneously satisfied if RuO_2 single crystals have uniaxial magnetic anisotropy with isotropic susceptibility within the *ab* plane. Thus, magnetic orders with a component of the Néel vector not parallel to the *c* axis, including Case III in Fig. 1, are incompatible with the data in Fig. 2. These measurements also rule out magnetic domains and field-induced reorientation of a Néel vector, as has been reported in thin film RuO_2 [19] and other rutile magnets [46].

To distinguish between Cases I and II, quantitative arguments that move beyond symmetry are necessary. It is well established that systems with local or itinerant collinear magnetic order exhibit a smaller magnetic susceptibility parallel to the Néel vector that approaches zero at 0 K and a larger, temperature-independent magnetic susceptibility perpendicular to the Néel vector for small magnetic fields [53,54].

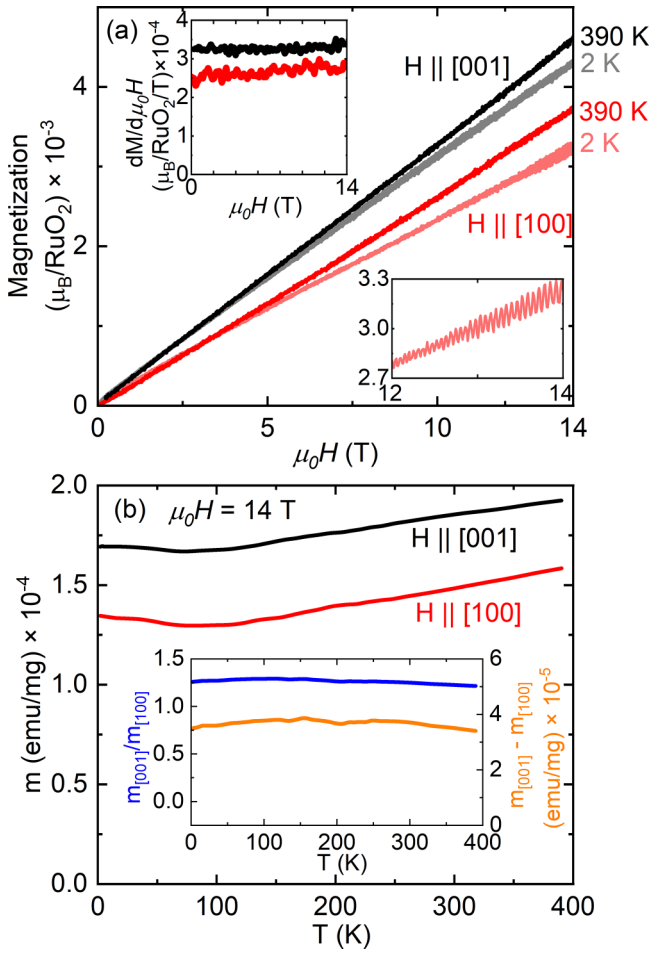

FIG. 3. (a) Longitudinal magnetization for different directions and temperatures. Quantum oscillations are present at high fields and low temperatures. Left inset: Differential susceptibility demonstrating linear-in-field magnetization. Right inset: Magnetic quantum oscillations when the field is along [100] at 2 K. (b) Temperature-dependent moment along different directions. Inset: Temperature dependence of $m_{[001]}/m_{[100]}$ and $m_{[001]}-m_{[100]}$ to quantify anisotropy.

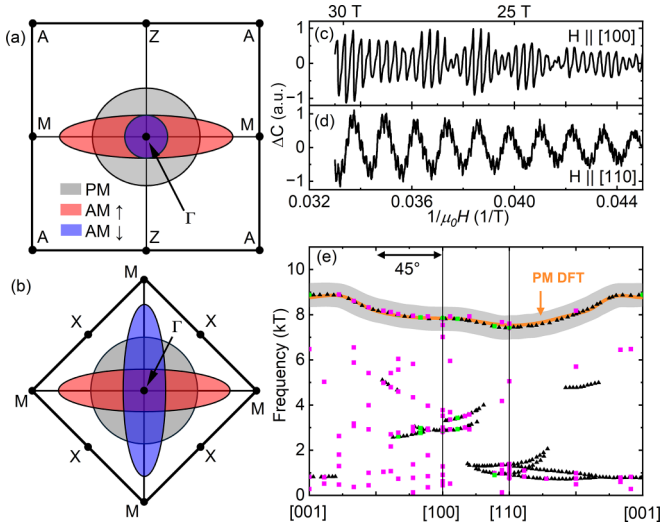

FIG. 4. Fermi surface of RuO_2. (a), (b) Sketches of the Fermi surface pocket at the Γ point along the (a) ΓM and (b) ΓZ directions assuming paramagnetism and altermagnetism. The pocket in the paramagnetic case is shown in gray. Blue and red depict the spin-split pocket in the presence of altermagnetic order. (c), (d) Examples of quantum oscillations measured with torque magnetometry at 0.5 K in two directions after a polynomial subtraction of the background. (e) Quantum oscillation frequencies with respect to magnetic field direction. Symbols denote different techniques (circles are magnetization, squares are torque magnetometry) and colors indicate different samples. Triangles are from prior work [56]. The highest frequencies, corresponding to a nearly spherical pocket around the Γ point (gray, shaded), show good agreement with DFT calculated quantum oscillation frequencies [48] for the Γ point pocket in paramagnetic RuO_2 (orange). See the Supplemental Material for further details on DFT comparison [50].

Therefore, one would expect $\chi_a > \chi_c$ with $\lim_{T\to 0} \chi_c = 0$ in Case II.

The first piece of evidence supporting paramagnetic Case I over altermagnetic Case II is the sign of the torque, which indicates $\chi_c > \chi_a$ (Fig. 2). To corroborate $\chi_c > \chi_a$ and check whether $\lim_{T\to 0} \chi_c = 0$, we measure the longitudinal magnetization along the a and c axes (Fig. 3). Both directions are dominated by linear-in-field magnetization at all temperatures (see the Supplemental Material [50]). The magnitudes of the magnetization along these two directions show a similar, weak temperature dependence such that the magnetic anisotropy minimally varies with temperature, in agreement with previous reports [38,55]. Consequently, the magnetization for a given magnetic field remains approximately 20% larger along the c axis at all temperatures, and the magnetic susceptibility does not tend toward zero in the limit of 0 K in either principal crystallographic direction.

Therefore, the magnetization data in Fig. 3 reinforce the torque evidence for paramagnetic Case I. In fact, the magnetic anisotropy $\chi_a - \chi_c$ determined from magnetization [2.4(2) × 10^{-5}] and torque [2.3(1) × 10^{-5}] are in quantitative agreement [50]. It is also worth noting our RuO_2 single crystal results quantitatively agree with other measurements on single crystals [38,55], but substantially differ from some RuO_2 thin film measurements [19,28]. First, we observe no phase transitions from 0.5–400 K and up to 31 T (thin films show a zero-field transition near 380 K [19]). Second, the susceptibilities in Fig. 3 are two orders of magnitude smaller than those reported for thin films [19]. Third, Fig. 2 shows no evidence for spin reorientation when a component of the magnetic field is along [110] up to 31 T, whereas this occurs at ∼1 T in thin films [19].

An additional stringent test for paramagnetic RuO_2 single crystals is characterizing the Fermi surface of RuO_2 because the magnetic properties of itinerant paramagnets reflect their Fermi surface. Furthermore, density functional theory (DFT) calculations indicate pronounced differences between paramagnetic and altermagnetic Fermi surfaces, particularly in the shape of the Brillouin zone center pocket: this pocket is nearly spherical for paramagnetic RuO_2, whereas it is flatter with a fourfold distortion reflecting d-wave altermagnetism in altermagnetic RuO_2 [Figs. 4(a) and 4(b)]. Table I quantifies predicted differences in the Fermi surface shape via ratios of the Γ point pocket radii along the ΓM, ΓZ, and ΓX paths. Although there is some scatter

TABLE I. Fermi surface anisotropy at the Γ point from our measurements, literature measurements, and literature DFT calculations assuming paramagnetism (Case I) and altermagnetism (Case II). Values are the ratios ΓM/ΓZ and ΓX/ΓM of the Γ point pocket (see the Supplemental Material for details [50]).

	Quantum oscillations (Exp.)	Paramagnetic (DFT)	Altermagnetic (DFT)
ΓM/ΓZ	1.12(1) [this work]	1.10 [48]	3.25 [48]
	1.23 [56]	0.91 [57]	1.53 [57]
			3.87 [59]
ΓX/ΓM	1.06(1) [this work]	1.05 [48]	0.36 [48]
	1.00 [56]	1.03 [57]	1.00 [57]
		1.10 [60]	0.71 [60]
			0.44 [61]
			0.2 [59]

in the altermagnetic DFT calculations, altermagnetic Fermi surfaces are significantly more anisotropic than paramagnetic Fermi surfaces.

We directly characterized the Fermi surface with quantum oscillations [47] measured by torque magnetometry [Figs. 4(c) and 4(d)] and magnetization [Fig. 3(a) and Supplemental Material [50]] to determine the shape of the Γ point pocket and distinguish between a paramagnetic and an altermagnetic Fermi surface. The principal features of the angular-dependent quantum oscillation frequencies in Fig. 4(e) are a set of high frequencies that vary minimally with angle (7.4–8.9 kT) and a range of lower frequencies with complex angular dependencies (see the Supplemental Material for details [50]). The former are associated with a nearly spherical Fermi surface pocket at the Brillouin zone center, and the latter are attributed to smaller, nonspherical pocket(s) [48,56,57]. These features agree well with previous measurements of quantum oscillations in RuO_2 single crystals [56,58]; however, we observed additional lower frequencies owing to the availability of higher fields and lower temperatures. Crucially, these measurements reveal a nearly spherical Γ point pocket (Fig. 4), which is in quantitative agreement with theoretical paramagnetic Fermi surfaces [Fig. 4(e) and Supplemental Material [50]]. Thus, the experimental Fermi surface of RuO_2 is consistent with paramagnetism, not altermagnetism.

Prior to recent measurements [25] and work on altermagnetism [61], the prevailing interpretation was RuO_2 is an itinerant paramagnet. For example, the Pauli paramagnetic susceptibility of RuO_2 determined from the Sommerfeld coefficient [62] semiquantitatively agrees with the measured magnetic susceptibility [38]. Our results are consistent with this interpretation and indicate high-quality, single crystals of RuO_2 are itinerant paramagnets. We reproduced our findings on multiple samples, instruments, and techniques (see Fig. 4 and Supplemental Material [50]) and confirmed sample quality by determining the electron mean free path (≈160 unit cells) and residual-resisitivity ratio (≈250). In addition to the symmetry of the magnetic susceptibility tensor, relative size of the magnetic susceptibility components, and shape of the Fermi surface, other observations in Figs. 2 and 3 are also consistent with itinerant paramagnetism: (1) $d\chi/dT > 0$ implies a local minimum in the electronic density of states at the Fermi level [63,64], in agreement with other RuO_2 work [62,65]; (2) the small, low-temperature upturns in χ_a and χ_c reflect contributions from multiple bands at the Fermi level [44,65–67]; and (3) the small magnitudes and weak temperature dependencies of χ_a and χ_c and nearly temperature-independent anisotropy are consequences of magnetization originating from spin polarization of the Fermi surface [68,69].

So what of altermagnetism in RuO_2? Our measurements indicate that high-quality RuO_2 single crystals are intrinsically paramagnets that do not exhibit long-range magnetic order, nor by extension spin splitting. These results are an important benchmark for future work on RuO_2 and strongly suggest that reports of magnetic order in RuO_2 have an extrinsic origin. Such an interpretation is supported by recent experiments showing the importance of epitaxial strain and thickness in inducing magnetic order in RuO_2 thin films [29] and calculations suggesting that point defects can drive RuO_2 toward a magnetic state [70]. As a result of this extrinsic nature, possible avenues to engineer and tailor altermagnetism in RuO_2 warrant further study. More generally, these results emphasize that torque magnetometry (in conjunction with magnetization) is a powerful approach to study anisotropy in compensated magnetic systems including putative altermagnets.

In summary, we have used a combination of thermodynamic probes to characterize magnetic order in high-quality RuO_2 single crystals. Our measurements indicate uniaxial anisotropy with isotropic magnetic susceptibility within the *ab* plane and $\chi_c > \chi_a$ up to 31 T at all investigated temperatures. Magnetic quantum oscillations demonstrate a nearly spherical Fermi surface pocket around the Brillouin zone center, in agreement with the theoretical paramagnetic Fermi surface. Together, these results strongly suggest that RuO_2 single crystals are intrinsically itinerant paramagnets without long-range magnetic order and, accordingly, not altermagnets.

Note added. After submission, we became aware of two recent works investigating altermagnetism [71] and the Fermi surface [72] of RuO_2 single crystals. Both studies reached similar conclusions.

Acknowledgments. T.Q., B.M., M.L., and C.A.M. acknowledge the support of the Laboratory Directed Research and Development program of Los Alamos National Laboratory under Project No. 20240225ER. A.R. and H.Z. acknowledge support from the U.S. Department of Energy with Grant No. DE-SC0020254. A portion of this work was performed at the National High Magnetic Field Laboratory, which is supported by the National Science Foundation Cooperative Agreement No. DMR-2128556, the State of Florida, and the Department of Energy. The authors thank Shermane Benjamin and Clyde Martin for technical assistance at the National High Magnetic Field Laboratory's DC Field Facility.

Data availability. The data are available upon reasonable request from the authors.

[1] A. S. Borovik Romanov, H. Grimmer, and M. Kenzelmann, Magnetic properties, in *International Tables for Crystallography* (John Wiley & Sons, Ltd, Hoboken, New Jersey, 2013), Chap. 1.5, pp. 106–152.

[2] A. Hirohata, K. Yamada, Y. Nakatani, I.-L. Prejbeanu, B. Diény, P. Pirro, and B. Hillebrands, Review on spintronics: Principles and device applications, J. Magn. Magn. Mater. **509**, 166711 (2020).

[3] T. Jungwirth, X. Marti, P. Wadley, and J. Wunderlich, Antiferromagnetic spintronics, Nat. Nanotechnol. **11**, 231 (2016).

[4] L. Šmejkal, J. Sinova, and T. Jungwirth, Beyond conventional ferromagnetism and antiferromagnetism: A phase with nonrelativistic spin and crystal rotation symmetry, Phys. Rev. X **12**, 031042 (2022).

[5] L. Šmejkal, J. Sinova, and T. Jungwirth, Emerging research landscape of altermagnetism, Phys. Rev. X **12**, 040501 (2022).

[6] D. B. Litvin and W. Opechowski, Spin groups, Physica **76**, 538 (1974).

[7] S. Bhowal and N. A. Spaldin, Ferroically ordered magnetic octupoles in *d*-wave altermagnets, Phys. Rev. X **14**, 011019 (2024).

[8] P. A. McClarty and J. G. Rau, Landau theory of altermagnetism, Phys. Rev. Lett. **132**, 176702 (2024).

[9] S. Hayami, Y. Yanagi, and H. Kusunose, Momentum-dependent spin splitting by collinear antiferromagnetic ordering, J. Phys. Soc. Jpn. **88**, 123702 (2019).

[10] L.-D. Yuan, Z. Wang, J.-W. Luo, E. I. Rashba, and A. Zunger, Giant momentum-dependent spin splitting in centrosymmetric low-*Z* antiferromagnets, Phys. Rev. B **102**, 014422 (2020).

[11] T. Jungwirth, R. M. Fernandes, E. Fradkin, A. H. MacDonald, J. Sinova, and L. Šmejkal, Altermagnetism: An unconventional spin-ordered phase of matter, Newton **1**, 100162 (2025).

[12] A. B. Hellenes, T. Jungwirth, R. Jaeschke-Ubiergo, A. Chakraborty, J. Sinova, and L. Šmejkal, *P*-wave magnets, arXiv:2309.01607.

[13] S.-W. Cheong and F.-T. Huang, Altermagnetism with noncollinear spins, npj Quantum Mater. **9**, 13 (2024).

[14] L.-D. Yuan, A. B. Georgescu, and J. M. Rondinelli, Nonrelativistic spin splitting at the Brillouin zone center in compensated magnets, Phys. Rev. Lett. **133**, 216701 (2024).

[15] C. Xu, S. Wu, G.-X. Zhi, G. Cao, J. Dai, C. Cao, X. Wang, and H.-Q. Lin, Altermagnetic ground state in distorted kagome metal $CsCr_3SB_5$, Nat. Commun. **16** (2025),.

[16] S. Reimers, L. Odenbreit, L. Šmejkal, V. N. Strocov, P. Constantinou, A. B. Hellenes, R. Jaeschke Ubiergo, W. H. Campos, V. K. Bharadwaj, A. Chakraborty, *et al.*, Direct observation of altermagnetic band splitting in CrSb thin films, Nat. Commun. **15**, 2116 (2024).

[17] T. Aoyama and K. Ohgushi, Piezomagnetic properties in altermagnetic MnTe, Phys. Rev. Mater. **8**, L041402 (2024).

[18] S. Lee, S. Lee, S. Jung, J. Jung, D. Kim, Y. Lee, B. Seok, J. Kim, B. G. Park, L. Šmejkal, *et al.*, Broken Kramers degeneracy in altermagnetic MnTe, Phys. Rev. Lett. **132**, 036702 (2024).

[19] Z. Feng, X. Zhou, L. Šmejkal, L. Wu, Z. Zhu, H. Guo, R. González-Hernández, X. Wang, H. Yan, P. Qin, *et al.*, An anomalous Hall effect in altermagnetic ruthenium dioxide, Nat. Electron. **5**, 735 (2022).

[20] M. Leiviskä, J. Rial, A. Bad'ura, R. L. Seeger, I. Kounta, S. Beckert, D. Kriegner, I. Joumard, E. Schmoranzerová, J. Sinova, *et al.*, Anisotropy of the anomalous Hall effect in thin films of the altermagnet candidate Mn_5Si_3, Phys. Rev. B **109**, 224430 (2024).

[21] H. Schäfer, G. Schneidereit, and W. Gerhardt, Zur chemie der platinmetalle. RO_2 chemischer transport, eigenschaften, thermischer zerfall, Z. Anorg. Allg. Chem. **319**, 327 (1963).

[22] K. Kameyama, K. Tsukada, K. Yahikozawa, and Y. Takasu, Surface characterization of RuO_2-IrO_2-TiO_2 coated titanium electrodes, J. Electrochem. Soc. **141**, 643 (1994).

[23] I. Bat'ko, K. Flachbart, M. Somora, and D. Vanický, Design of RuO_2-based thermometers for the millikelvin temperature range, Cryogenics **35**, 105 (1995).

[24] H. Over, Y. D. Kim, A. P. Seitsonen, S. Wendt, E. Lundgren, M. Schmid, P. Varga, A. Morgante, and G. Ertl, Atomic-scale structure and catalytic reactivity of the RuO_2 (110) surface, Science **287**, 1474 (2000).

[25] T. Berlijn, P. C. Snijders, O. Delaire, H.-D. Zhou, T. A. Maier, H.-B. Cao, S.-X. Chi, M. Matsuda, Y. Wang, M. R. Koehler, *et al.*, Itinerant antiferromagnetism in RuO_2, Phys. Rev. Lett. **118**, 077201 (2017).

[26] P. Keßler, L. Garcia-Gassull, A. Suter, T. Prokscha, Z. Salman, D. Khalyavin, P. Manuel, F. Orlandi, I. I. Mazin, R. Valentí, *et al.*, Absence of magnetic order in RuO_2: Insights from μSR spectroscopy and neutron diffraction, npj Spintron. **2**, 50 (2024).

[27] Z. H. Zhu, J. Strempfer, R. R. Rao, C. A. Occhialini, J. Pelliciari, Y. Choi, T. Kawaguchi, H. You, J. F. Mitchell, Y. Shao-Horn, and R. Comin, Anomalous antiferromagnetism in metallic RuO_2 determined by resonant x-ray scattering, Phys. Rev. Lett. **122**, 017202 (2019).

[28] T. Tschirner, P. Keßler, R. D. Gonzalez Betancourt, T. Kotte, D. Kriegner, B. Büchner, J. Dufouleur, M. Kamp, V. Jovic, L. Smejkal, *et al.*, Saturation of the anomalous Hall effect at high magnetic fields in altermagnetic RuO_2, APL Mater. **11**, 101103 (2023).

[29] S. G. Jeong, S. Lee, B. Lin, Z. Yang, I. H. Choi, J. Y. Oh, S. Song, S. wook Lee, S. Nair, R. Choudhary, J. Parikh, S. Park, W. S. Choi, J. S. Lee, J. M. LeBeau, T. Low, and B. Jalan, Metallicity and anomalous Hall effect in epitaxially strained, atomically thin RuO_2 films, Proc. Natl. Acad. Sci. USA **122**, e2500831122 (2025).

[30] S. Karube, T. Tanaka, D. Sugawara, N. Kadoguchi, M. Kohda, and J. Nitta, Observation of spin-splitter torque in collinear antiferromagnetic RuO_2, Phys. Rev. Lett. **129**, 137201 (2022).

[31] H. Bai, Y. C. Zhang, Y. J. Zhou, P. Chen, C. H. Wan, L. Han, W. X. Zhu, S. X. Liang, Y. C. Su, X. F. Han, F. Pan, and C. Song, Efficient spin-to-charge conversion via altermagnetic spin splitting effect in antiferromagnet RuO_2, Phys. Rev. Lett. **130**, 216701 (2023).

[32] X. Feng, H. Bai, X. Fan, M. Guo, Z. Zhang, G. Chai, T. Wang, D. Xue, C. Song, and X. Fan, Incommensurate spin density wave in antiferromagnetic RuO_2 evinced by abnormal spin splitting torque, Phys. Rev. Lett. **132**, 086701 (2024).

[33] M. Weber, S. Wust, L. Haag, A. Akashdeep, K. Leckron, C. Schmitt, R. Ramos, T. Kikkawa, E. Saitoh, M. Kläui, *et al.*, All optical excitation of spin polarization in *d*-wave altermagnets, arXiv:2408.05187.

[34] S. G. Jeong, I. H. Choi, S. Nair, L. Buiarelli, B. Pourbahari, J. Y. Oh, N. Bassim, D. Hirai, A. Seo, W. S. Choi, R. M. Fernandes, T. Birol, L. Zhao, J. S. Lee, and B. Jalan, Altermagnetic polar metallic phase in ultra-thin epitaxially-strained RuO_2 films, arXiv:2405.05838.

[35] J. Liu, J. Zhan, T. Li, J. Liu, S. Cheng, Y. Shi, L. Deng, M. Zhang, C. Li, J. Ding, *et al.*, Absence of altermagnetic spin splitting character in rutile oxide RuO_2, Phys. Rev. Lett. **133**, 176401 (2024).

[36] E. H. P. Cordfunke, R. J. M. Konings, E. F. Westrum, Jr., and R. Shaviv, The thermophysical and thermochemical properties of RuO_2 from 0 to 1000 K, J. Phys. Chem. Solids **50**, 429 (1989).

[37] H. St. C. O'Neill and J. Johan, Gibbs free energies of formation of RuO_2, IrO_2, and OsO_2: A high-temperature electrochemical and calorimetric study, Geochim. Cosmochim. Acta **61**, 5279 (1997).

[38] W. D. Ryden and A. W. Lawson, Magnetic susceptibility of IrO_2 and RuO_2, J. Chem. Phys. **52**, 6058 (1970).

[39] J. M. Fletcher, W. E. Gardner, B. F. Greenfield, M. J. Holdoway, and M. H. Rand, Magnetic and other studies of ruthenium dioxide and its hydrate, J. Chem. Soc. A: Inorg. Phys. Theor. 653 (1968).

[40] J.-J. Lin, S. M. Huang, Y. H. Lin, T. C. Lee, H. Liu, X. X. Zhang, R. S. Chen, and Y. S. Huang, Low temperature electrical transport properties of RuO_2 and IrO_2 single crystals, J. Phys.: Condens. Matter **16**, 8035 (2004).

[41] K. M. Glassford and J. R. Chelikowsky, Electron transport properties in RuO_2 rutile, Phys. Rev. B **49**, 7107 (1994).

[42] Y. S. Touloukian, R. K. Kirby, E. R. Taylor, and T. Y. Lee, *Thermophysical Properties of Matter—The TPRC Data Series. Thermal Expansion—Nonmetallic Solids.(Reannouncement). Data book*, Technical Report (Purdue University, Lafayette, IN, 1977).

[43] M. Hiraishi, H. Okabe, A. Koda, R. Kadono, T. Muroi, D. Hirai, and Z. Hiroi, Nonmagnetic ground state in RuO_2 revealed by muon spin rotation, Phys. Rev. Lett. **132**, 166702 (2024).

[44] F. Pawula, A. Fakih, R. Daou, S. Hébert, N. Mordvinova, O. Lebedev, D. Pelloquin, and A. Maignan, Multiband transport in RuO_2, Phys. Rev. B **110**, 064432 (2024).

[45] M. Wenzel, E. Uykur, S. Rößler, M. Schmidt, O. Janson, A. Tiwari, M. Dressel, and A. A. Tsirlin, Fermi-liquid behavior of nonaltermagnetic RuO_2, Phys. Rev. B **111**, L041115 (2025).

[46] A. Bazhan and C. Bazan, Weak ferromagnetism in CoF_2 and NiF_2, J. Exp. Theor. Phys. **42**, 898 (1975).

[47] D. Shoenberg, *Magnetic Oscillations in Metals* (Cambridge University Press, Cambridge, 1984).

[48] Y. Huang, J. Lai, J. Zhan, T. Yu, R. Chen, P. Liu, X.-Q. Chen, and Y. Sun, *Ab initio* study of quantum oscillations in altermagnetic and nonmagnetic phases of RuO_2, Phys. Rev. B **110**, 144410 (2024).

[49] J. M. Pérez-Mato, S. V. Gallego, E. S. Tasci, L. Elcoro, G. de la Flor, and M. I. Aroyo, Symmetry-based computational tools for magnetic crystallography, Annu. Rev. Mater. Res. **45**, 217 (2015).

[50] See Supplemental Material at http://link.aps.org/supplemental/10.1103/s98c-nkgj for additional experimental details and measurements on multiple samples, which includes Refs. [62,73].

[51] M. Perfetti, Cantilever torque magnetometry on coordination compounds: From theory to experiments, Coord. Chem. Rev. **348**, 171 (2017).

[52] T. Komatsubara, M. Murakami, and E. Hirahara, Magnetic properties of manganese telluride single crystals, J. Phys. Soc. Jpn. **18**, 356 (1963).

[53] S. Blundell, *Magnetism in Condensed Matter* (Oxford University Press, Oxford, 2001).

[54] A. B. Lidiard, Antiferromagnetism in metals, Proc. R. Soc. A **224**, 161 (1954).

[55] L. Kiefer, F. Wirth, A. Bertin, P. Becker, L. Bohatý, K. Schmalzl, A. Stunault, J. A. Rodríguez-Velamazan, O. Fabelo, and M. Braden, Crystal structure and absence of magnetic order in single-crystalline RuO_2, J. Phys.: Condens. Matter **37**, 135801 (2025).

[56] J. E. Graebner, E. S. Greiner, and W. D. Ryden, Magnetothermal oscillations in RuO_2, OsO_2, and IrO_2, Phys. Rev. B **13**, 2426 (1976).

[57] K.-H. Ahn, A. Hariki, K.-W. Lee, and J. Kuneš, Antiferromagnetism in RuO_2 as d-wave Pomeranchuk instability, Phys. Rev. B **99**, 184432 (2019).

[58] S. M. Marcus and S. R. Butler, Measurement of the de Haas-van Alphen effect in the rutile structure RuO_2, Phys. Lett. A **26**, 518 (1968).

[59] K. Samanta, Y.-Y. Jiang, T. R. Paudel, D.-F. Shao, and E. Y. Tsymbal, Tunneling magnetoresistance in magnetic tunnel junctions with a single ferromagnetic electrode, Phys. Rev. B **109**, 174407 (2024).

[60] O. Fedchenko, J. Minár, A. Akashdeep, S. W. D'Souza, D. Vasilyev, O. Tkach, L. Odenbreit, Q. Nguyen, D. Kutnyakhov, N. Wind, *et al.*, Observation of time-reversal symmetry breaking in the band structure of altermagnetic RuO_2, Sci. Adv. **10**, eadj4883 (2024).

[61] L. Šmejkal, R. Gonzalez-Hernandez, T. Jungwirth, and J. Sinova, Crystal time-reversal symmetry breaking and spontaneous Hall effect in collinear antiferromagnets, Sci. Adv. **6**, eaaz8809 (2020).

[62] K. M. Glassford and J. R. Chelikowsky, Electronic and structural properties of RuO_2, Phys. Rev. B **47**, 1732 (1993).

[63] E. C. Stoner, Collective electron specific heat and spin paramagnetism in metals, Proc. R. Soc. A **154**, 656 (1936).

[64] C. J. Kriessman and H. B. Callen, The magnetic susceytibility of the transition elements, Phys. Rev. **94**, 837 (1954).

[65] P. A. Cox, J. B. Goodenough, P. J. Tavener, D. Telles, and R. G. Egdell, The electronic structure of $Bi_{2-x}Gd_xRu_2O_7$ and RuO_2: A study by electron spectroscopy, J. Solid State Chem. **62**, 360 (1986).

[66] M. Shimizu and T. Takahashi, Magnetic susceptibilities of nonferromagnetic transition metals, J. Phys. Soc. Jpn. **15**, 2236 (1960).

[67] L. F. Mattheiss, Electronic structure of RuO_2, OsO_2, and IrO_2, Phys. Rev. B **13**, 2433 (1976).

[68] É. V. Galoshina, Magnetic susceptibility of d-band transition metals that are not magnetically ordered, Sov. Phys. Usp. **17**, 345 (1974).

[69] M. Shimizu, Itinerant electron magnetism, Rep. Prog. Phys. **44**, 329 (1981).

[70] A. Smolyanyuk, I. I. Mazin, L. Garcia-Gassull, and R. Valentí, Fragility of the magnetic order in the prototypical altermagnet RuO_2, Phys. Rev. B **109**, 134424 (2024).

[71] G. Yumnam, P. R. Raghuvanshi, J. D. Budai, L. Bocklage, D. Abernathy, Y. Cheng, A. H. Said, I. I. Mazin, H. Zhou, B. A. Frandsen, D. S. Parker, L. R. Lindsay, V. R. Cooper, M. E. Manley, and R. P. Hermann, Constraints on magnetism and correlations in RuO_2 from lattice dynamics and Mössbauer spectroscopy, Cell Rep. Phys. Sci. **6**, 102852 (2025).

[72] Z. Wu, M. Long, H. Chen, S. Paul, H. Matsuki, O. Zheliuk, U. Zeitler, G. Li, R. Zhou, Z. Zhu, D. Graf, T. I. Weinberger, F. M. Grosche, Y. Maeno, and A. G. Eaton, Fermi surface of RuO_2 measured by quantum oscillations, Phys. Rev. X **15**, 031044 (2025).

[73] L. D. Landau, L. Pitaevskii, A. M. Kosevich, and E. M. Lifshitz, *Theory of Elasticity* (Elsevier, 2012), Vol. 7.